Nonplanar Conformers and the Phase Behavior of Solid *n*-Alkanes

Mark Maroncelli, Song Ping Qi, Herbert L. Strauss,* and Robert G. Snyder*

Contribution from the Department of Chemistry, University of California, Berkeley California 94720. *Received January 21, 1982*

Abstract: Solid–solid phase transitions of the odd *n*-alkanes n-$C_{17}H_{36}$ through n-$C_{29}H_{60}$ were studied by using differential scanning calorimetry (DSC) and infrared (IR) spectroscopy. Two phase transitions were found in C_{25}, C_{27}, and C_{29} in addition to the previously reported highest-temperature solid–solid transition (the so-called "rotator" transition). IR spectra revealed that, as the temperature is raised, the concentration of nonplanar conformers successively increases through *each* phase transition. Three types of nonplanar defects have been identified in the highest-temperature phase of all the *n*-alkanes: "end-gauche" (gt...), "kink" (...gtg'...), and "double-gauche" (...gg...). The end-gauche defect was observed in the lower-temperature phases as well. Kink conformers, however, were observed only in the highest-temperature phase while double-gauche defects were found in measurable concentrations only within a few degrees of the melting point. The concentrations of nonplanar conformers in the highest-temperature phases increase with increasing chain length. For example, roughly 70% of C_{29} molcules are nonplanar prior to melting, in contrast to 5–10% for C_{17}. The relationship between the existence of nonplanar conformers and the various distinct solid phases presents a major puzzle.

Introduction

Normal alkanes undergo a remarkable series of solid–solid phase transitions prior to melting. Analogous premelting transitions are also found in a number of more complex systems which contain hydrocarbon chains as major constituents. These systems include polyethylene,[1] variously substituted alkanes,[2] and biological membranes.[3] In the latter cases, the phase changes are believed to be intimately related to the state of the hydrocarbon component. For example, current models of the lipid bilayer phase transitions require detailed consideration of the changes in conformation of the alkane chains.[4] Since the *n*-alkanes themselves are the simplest of these chain-molecule solids, they are a natural starting point for understanding the premelting transitions exhibited by all of these systems.

The phase behavior of even the *n*-alkanes is complex. All odd *n*-alkanes between C_9 and C_{45} undergo at least one premelting phase transition, and the longer members show no less than four high-temperature solid phases in addition to the low-temperature crystalline phase.[5] The nature of these phases is not well understood although it is clear that the higher-temperature phases involve increasing degrees of disorder. By disorder here we mean any deviation from the regular arrangement of all-trans chains found in the low-temperature solid.

In this paper we focus mainly on one aspect of the disordering processes occurring in these solids—that involving conformational changes. We show that infrared spectroscopy is sensitive to the presence of various nonplanar (not all-trans) conformers and to some types of intermolecular order. We will find that "disorder" occurs in a series of apparently solid phases. The question then arises how can the apparent short-range disorder implied by these nonplanar conformations be reconciled with the existence of a series of phases showing long-range order? This question which is fundamental to the understanding of the more complex systems such as biolipid bilayers will be taken up again in the Conclusion. The body of this paper presents the infrared spectra of the alkanes as a function of temperature with an analysis of the conformational "defects" seen in the various phases.

Background

The low-temperature crystal structures of odd and even *n*-alkanes differ. In this paper we consider only the odd *n*-alkanes since members having more than nine carbon atoms form a single homologous series and show virtually identical packing at low temperatures.[6,7] In this state, the molecules exist in the fully extended or all-trans conformation. The molecules are arranged in layers in which the chain axes are parallel to each other and perpendicular to the surface of the layer. The unit cell is orthorhombic and contains two molecules within each layer.

Müller[8] first observed that many *n*-alkanes undergo a solid–solid phase transition within a few degrees of their melting points. Using X-ray diffraction methods he found that, at the transition, the lateral unit cell dimensions changed so as to approach hexagonal symmetry. (True hexagonal symmetry is achieved only by chains longer than C_{21}.[9]) Noting that a hexagonal arrangement is the closest packing of cylinders, Müller proposed that, at the transition, molecules become effectively cylindrical as a result of executing rotation-like motions about their long axes.

Subsequently it has been found that this premelting phase transition occurs for all odd *n*-alkanes between C_9 and C_{45}.[7] There have been many studies of the high-temperature phase, most of which have employed techniques such as NMR,[10] inelastic neutron scattering,[11] or dielectric absorption[12] that tend to emphasize the motional aspects of the phase transition. The results obtained with such methods have generally supported Müller's original model in which the high-temperature phase is characterized by orientational disorder. Thus, molecules are envisioned to execute more or less complicated rotational jumps about their long axes while maintaining a fully extende conformation. A number of extended theoretical studies based on this picture[13] have been moderately successful in accounting for available thermodynamic data. As a result, this rotational model has found widespread

(1) D. C. Bassett and B. Turner, *Nature (London), Phys. Sci.*, **240**, 146 (1972).
(2) For example: (a) *n*-alkylammonium salts, J. Tsau and D. F. R. Gilson, *J. Phys. Chem.*, **72**, 4082 (1968); (b) *n*-alkylcarboxylic acids, M. R. Barr, B. A. Dunell, and R. F. Grant, *Can. J. Chem.*, **41**, 1188 (1963).
(3) S. C. Chen, J. M. Sturdevant, and B. J. Gaffney, *Proc. Natl. Acad. Sci. U.S.A.*, **77**, 5060 (1980).
(4) J. F. Nagle, *Annu. Rev. Phys. Chem.*, **31**, 157 (1980), and references therein.
(5) R. G. Snyder, M. Maroncelli, S. P. Qi, and H. L. Strauss, *Science*, **214**, 188 (1981).
(6) A. E. Smith, *J. Chem. Phys.*, **21**, 2229 (1953).
(7) M. G. Broadhurst, *J. Res. Natl. Bur. Stand., Sect. A*, **66**, 241 (1962).
(8) A. Müller, *Proc. R. Soc. London, Ser. A*, **138**, 514 (1932).
(9) J. Doucet, I. Denicolo, A. Craievich, and A. Collet, *J. Chem. Phys.*, **75**, 5125 (1981); J. Doucet, I. Denicolo, and A. Craievich, *ibid.*, **75**, 1523 (1981).
(10) R. E. Dehl, *J. Chem. Phys.*, **60**, 339 (1973); H. G. Olf and A. Peterlin, *J. Polym. Sci., Part A-2*, **8**, 791 (1970), and references therein.
(11) D. H. Bonsor, J. F. Barry, M. W. Newberry, M. V. Smalley, E. Granzer, C. Koberger, P. H. Nedwed, and J. Scheidel, *Chem. Phys. Lett.*, **62**, 576 (1979); D. Bloor, D. H. Bonsor, D. N. Batchelder, and C. G. Windsor, *Mol. Phys.*, **34**, 934 (1977); J. D. Barnes, *J. Chem. Phys.*, **58**, 5193 (1973).
(12) J. D. Hoffman, *J. Chem. Phys.*, **20**, 541 (1952).
(13) T. Ishinabe, *J. Chem. Phys.*, **72**, 353 (1980); M. Kobayashi, *ibid.*, **68**, 145 (1977); D. W. McClure, *ibid.*, **49**, 1830 (1968), and references cited therein.

0002-7863/82/1504-6237$01.25/0

acceptance and, in fact, the high-temperature phases of *n*-alkanes and similar compounds are often termed "rotator" phases.

Notably absent in this rotator model is any consideration of the possible role of conformational disorder. An alternative model, which focuses entirely on conformational disorder, was proposed by Pechhold and Blasenbrey.[14] These authors demonstrated that a number of observed properties of the rotator phase could be explained by postulating the existence of specific conformational defects which they termed "kinks". Such kink defects have received considerable attention in theoretical studies of polymers and lipid systems. This has not been the case, however, for the *n*-alkanes. Here the simple rotator model in which conformational effects are ignored has been favored.[15]

Recent studies have pointed out the inadequacy of the rotator model as a complete description of the premelting phase behavior of the *n*-alkanes. Strobl and co-workers[16] have found that the highest-temperature (rotator) phase of C_{33} is arrived at through a succession of at least three distinct phase transitions, rather than in a single step as was previously believed. Multiple phase transitions were also observed for the *n*-alkanes C_{31}, C_{37}, and C_{45} by Oyama et al.[17] The existence of several high-temperature phases in these longer *n*-alkanes indicates that more than one mechanism is involved in the disordering that occurs before melting.

In addition to demonstrating multiple phase transitions, Strobl and co-workers[16] have provided indirect evidence that the so-called rotator phase may involve a large fraction of molecules in nonplanar conformations. Strobl et al. estimated that as many as 40–70% of the molecules of C_{33} are nonplanar in the highest-temperature phase. This estimate is based on small-angle X-ray scattering measurements and assumes the existence of the kink defects proposed by Blasenbrey and Pechhold. Most recently, a spectroscopic study of Zerbi et al.[18] has provided evidence for the presence of gauche bonds near the ends of C_{19} in its high-temperature phase. These studies indicate that conformational changes are indeed an important contributing mechanism in the phase transitions—especially for longer *n*-alkanes.

Recently we have studied the odd *n*-alkanes C_{17}–C_{29} by means of infrared (IR) spectroscopy and, to a lesser extent, by differential scanning calorimetry (DSC). A preliminary account of this work has appeared.[5] For the longer members of this series, our DSC measurements reveal multiple solid phase transitions at temperatures that are consistent with those found for other *n*-alkanes by Strobl et al. and Oyama et al. We observe discontinuous changes in the IR spectra that occur exactly at the DSC transition temperatures. These changes reflect an increase in the number of nonplanar conformers as the melting point is approached. From an analysis of the new bands appearing in the spectra of the high-temperature phases, we have been able to ascertain the presence of certain specific conformational "defects". The magnitudes of the observed spectral changes indicate a high concentration of these defects prior to melting.

Experimental Section

The *n*-alkane samples were obtained from two sources. The series between C_{19} and C_{29} have been previously described by Schaerer et al.[19]

Table I. Transition Temperatures (in °C) Determined from DSC Measurements

n	T_{mp}[a]	T_α[a]	T_γ	T_δ
19	32.0	22.8 (22.8)		
21	40.2	32.6 (32.5)		
23	47.5	40.4 (40.5)		
25	53.5	46.7 (47.0)	46[b]	37.1
27	58.8	53.3 (53.0)	47.6 (47.1)[c]	36.6
29	63.4	57.9 (58.2)	49.2	37.0

[a] Values of T_{mp} and the T_α values given in parentheses are from ref 7. These values of T_{mp} were used to calibrate our measurements. [b] DSC scans did not separate the γ and α transitions for C_{25}. However, IR measurements indicate that γ and α may be partially separable. [c] Schaerer et al.[19] have previously observed the γ transition in C_{27} and the value in parentheses here refers to their value.

Table II. Transition Enthalpies (ΔH, in kcal/mol)

n	ΔH_{mp}[a]	ΔH_α[a]	ΔH_γ	ΔH_δ
19	10.95	3.2 (3.30)		
21	11.4	4.1 (3.7)		
23	12.9	5.6 (5.2)		
25[b]	13.8	6.8 (6.2)		0.08
27	14.44	6.5 (6.35)[c]	0.58 (0.57)[c]	0.07
29	15.80	7.2 (7.54)	0.62	0.07

[a] Values of ΔH_{mp} and the ΔH_α values given in parentheses are from ref 7. These values of ΔH_{mp} were used to calibrate our measurements. [b] For C_{25} ΔH_α also includes the contribution from ΔH_γ. [c] Reference 19.

Mass-spectral analysis indicated a purity of 99.6–99.9 mol %. The sample of n-$C_{17}H_{36}$ was obtained from Aldrich Chemicals with a stated purity >99 mol % and was used as received.

Calorimetric measurements were made with a Perkin-Elmer Model DSC-2 differential scanning calorimeter. Transition temperatures and approximate enthalpies of the solid–solid transitions were established by comparison with values reported[7] for the temperatures and enthalpies of fusion for these compounds.

Infrared spectra were measured with an evacuatable Nicolet Model 8000 FT IR spectrometer equipped with a TGS and a cooled MCT/InSb infrared detector. All spectra were recorded with operating parameters chosen to provide a resolution of $\sim$1 cm^{-1}. Most of the conformationally sensitive bands in the IR spectra are weak and therefore thick samples were needed. These consisted of $\sim$200-μm thick films sandwiched between NaCl windows. Such sandwiches were prepared by warming the solid *n*-alkane between windows to within a few degrees of the melting point of the sample at which temperature a thick low-scattering film could be formed. The sample was then cooled slowly and stored for several days at room temperature to help ensure equilibration.

The temperature of the sample was controlled as follows. The NaCl sandwich containing the sample was held in a cylindrical copper holder which fitted into an outer copper block. Except for the small optical ports, this outer block was wrapped on all sides with copper tubing soldered in place. The temperature of this assembly was regulated by circulating water or alcohol through the tubing from a thermostated bath. Sample temperatures were measured with a calibrated thermistor mounted inside the copper block. With this arrangement, sample temperatures could be regulated to ±0.02 °C with an estimated overall accuracy of ±0.1 °C.

The temperature of the sample was increased in steps with spectra being measured at each step. The time between successive measurements was approximately 0.5 h, and interval which we have found to be more than sufficient for temperature and phase equilibration of the sample.

Differential Scanning Calorimetry Results

Calorimetric data on the *n*-alkanes available prior to about 1962 have been summarized by Broadhurst.[7] In this critical review, the temperatures and enthalpies of the melting and main solid–solid (rotator) transitions were tabulated. The existence of other solid–solid phase transitions has been reported only recently and then only for *n*-alkanes longer than C_{31}. Therefore, we have made preliminary DSC measurements on the series of *n*-alkanes, C_{19}–C_{29}

(14) S. Blasenbrey and W. Pechhold, *Rheol. Acta*, **6**, 174 (1967).

(15) Actually one early study by J. D. Barnes and B. M. Fanconi (*J. Chem. Phys.*, **56**, 5190 (1972)) was designed to test the "kink-block" model of Blasenbrey and Pechhold. On the basis of their measured Raman spectra of C_{19}, Barnes and Fanconi reported that the large concentration of gauche bonds (they state four to eight per molecule) required by this model was not present in the high-temperature phase and that kink-block processes were therefore unlikely to be important in the "rotator" transition. Our own Raman spectra of C_{21} indicate that, although gauche concentrations are less than four per molecule, they are not negligible.

(16) B. Ewen, G. R. Strobl, and D. Richter, *Faraday Discuss. Chem. Soc.*, **69**, 19 (1980); G. Strobl, B. Ewen, E. W. Fischer, and W. Piesczek, *J. Chem. Phys.*, **61**, 5257 (1974); B. Ewen, E. W. Fischer, W. Piesczek, and G. Strobl, *ibid.*, **61**, 5265 (1974).

(17) T. Oyama, K. Takamizawa, and Y. Ogawa, *Kobunshi Ronbunshu*, **37**, 711 (1980); T. Oyama, K. Takamizawa, Y. Urabe, and Y. Ogawa, *Kyushu Daigaka Kogaku Shuho*, **52**, 129 (1979).

(18) G. Zerbi, R. Magni, M. Gussoni, K. H. Moritz, A. Bigotto, and S. Dirlikov, *J. Chem. Phys.*, **75**, 3175 (1981).

(19) A. A. Schaerer, C. J. Busso, A. E. Smith, and L. B. Skinner, *J. Am. Chem. Soc.*, **77**, 2017 (1955).

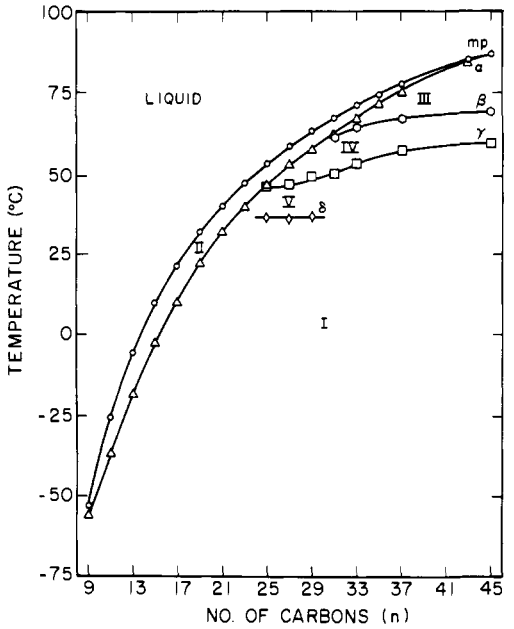

Figure 1. Transition temperatures of odd *n*-alkanes, C_n. The related transitions of different *n*-alkanes have been connected on the basis of similarity in the temperatures and enthalpies of transition. The solid–solid transition curves α, β, γ, and δ separate phases I, II, III, IV, and V. Data are from ref 7, 16, 17, and the present study. See also footnote 20 and Table I.

A more complete investigation of these *n*-alkanes is currently being undertaken.

For the shorter *n*-alkanes, C_{19}–C_{23}, we found only the so-called rotator transition. We designate this as the α transition. The longer *n*-alkanes, C_{25}–C_{29}, undergo two additional transitions at lower temperatures which we designate as γ and δ. The observed transition temperatures, which are summarized in Table I, were measured by using the melting points of the samples as an internal reference. For comparison, values of T_α given by Broadhurst[7] are also listed. The agreement between the two sets is within the estimated uncertainty (±0.5 °C) of our measurements.

We observed hysteresis upon cooling the samples. Measured values of T_{mp} and T_α were respectively 0.5 and 1–2 °C lower while the other transitions were lower by more than 5 °C.

The measured enthalpies of the solid–solid transitions are listed in Table II. Relative values were estimated from the areas of peaks in the DSC curves, and these were calibrated with the enthalpies of fusion compiled by Broadhurst.[7] Estimated uncertainties in these values are approximately ±10% for ΔH_α and ΔH_γ and ±30% for ΔH_δ. The α transition of the longer *n*-alkanes involves about half of enthalpy of fusion. However, the enthalpies associated with the lower-temperature transitions of these same *n*-alkanes are much smaller—ΔH_γ is about 4% of ΔH_{mp}, and ΔH_δ is about 0.5% of ΔH_{mp}.

The transition temperatures of the odd *n*-alkanes are summarized in Figure 1, where we have plotted transition temperatures as a function of chain length using data obtained in this study together with those of Broadhurst,[7] Strobl et al.,[16] and Oyama et al.[17] In this diagram, we have connected transitions that appear related on the basis of their temperatures and enthalpies. There are at least four distinct solid–solid transitions, thus requiring the existence of at least five different solid phases.[20] We denote the transitions by Greek letters and the phases by Roman numerals.

As noted, our DSC solid–solid phase transition data for C_{19}–C_{29} correlate with reported data on other alkanes. Thus, the transition observed in C_{25}–C_{29} which we have designated γ (Figure 1) appears to be the A → B transition reported for longer chains in ref 16 and 17. We note that at C_{31} the temperature of the β transition coincides with that of the α transition. As a consequence the β transition is not present for the shorter chains. The weak δ transition, which was first reported in our earlier communication,[5] has not been observed for the longer *n*-alkanes.

(20) The correspondence between phase designations used here and those of ref 7, 16, and 17 is as follows:

this work	ref 7	ref 16	ref 17
I	β_O	A	A
V			
IV		B	B
III		C	C
II	α_H	D	α

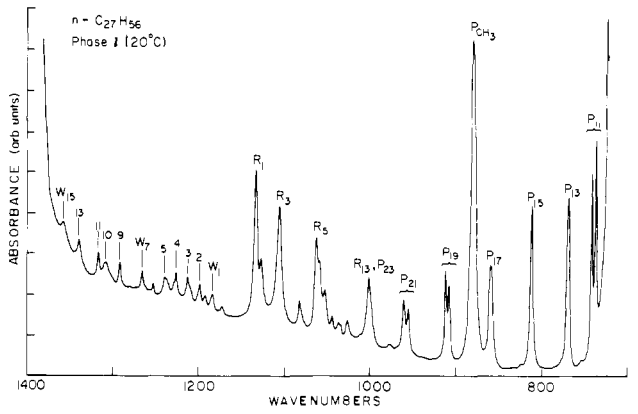

Figure 2. Infrared spectrum of n-$C_{27}H_{56}$ in phase I (20 °C). Some bands of three progressions are labeled: methylene rocking, P_k; the methylene wagging, W_k; and C–C stretching, R_k. P_{CH_3} denotes the methyl rocking mode. Assignments are from ref 22.

Infrared Spectra Results

Discussion of the results of the IR measurements is divided into four parts. In section A we discuss the relation between the IR spectra of the *n*-alkanes and their conformation and describe the differences between the spectra of the lowest-temperature phase (I) and the highest-temperature phase (II). In section B we discuss the normal coordinate calculations which enable us to assign those bands that appear in the spectrum of phase II but not phase I to specific nonplanar conformations. In section C we consider the differences in the concentrations of these nonplanar forms as a function of chain length. In section D we describe the spectra of the solid phases IV and V and discuss changes in spectra and structure as a function of temperature.

A. Infrared Spectra of Phases I and II. Studies of the vibrational spectra of *n*-alkanes in their lowest-temperature crystalline form (phase I) have led to a detailed understanding of the normal modes of the all-trans conformation of these molecules.[21,22] These studies have provided the foundation for the extension of the vibrational analysis to include the nonplanar conformations present in the liquid[23] as well as in the high-temperature solid phases of concern here.

Figure 2 illustrates the prominent features of the low-temperature-phase (I) IR spectrum in the conformationally sensitive region between 1400 and 700 cm^{-1}. This spectrum, which is of C_{27}, is representative of the phase I spectra of all of the odd *n*-alkanes. Essentially all the vibrations observed can be assigned to molecules that have the all-trans conformation.

In discussing the spectra of the *n*-alkanes, it is useful to classify vibrations into two types. First, there are vibrations which are nonlocalized and involve the entire chain. These nonlocalized modes give rise to band progressions which account for nearly all bands observed in this region of the IR spectrum. Three such progressions are shown in Figure 2—the methylene rocking (or rocking–twisting[21]) progression, labeled P_k; the wagging progression, W_k; and the C–C stretching progression, R_k. The integer subscript k which is used to label each mode in a progression is

(21) R. G. Snyder and J. H. Schachtschneider, *Spectrochim. Acta*, **19**, 85 (1963); J. H. Schachtschneider and R. G. Snyder, *ibid.*, **19**, 117 (1963).
(22) R. G. Snyder, *J. Mol. Spectrosc.*, **4**, 411 (1960); **7**, 116 (1961).
(23) R. G. Snyder, *J. Chem. Phys.*, **47**, 1316 (1967).

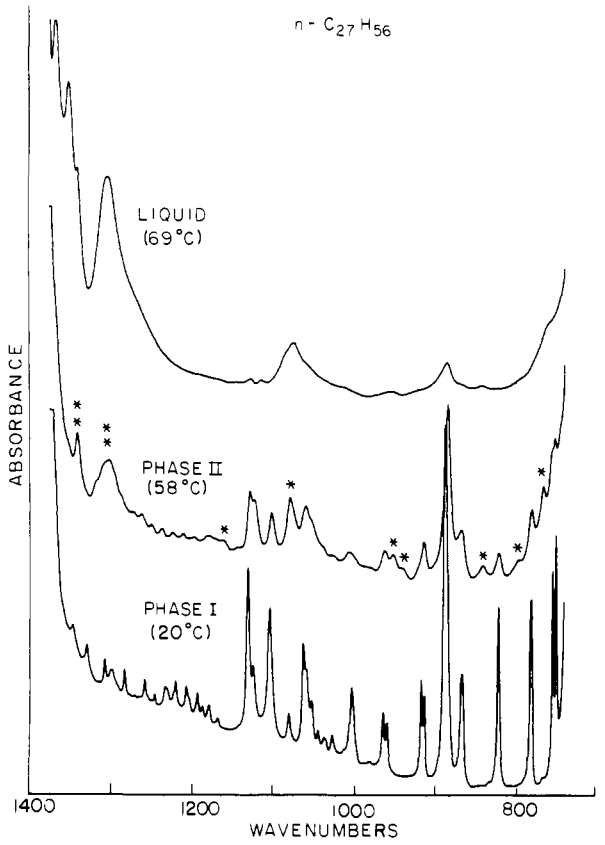

Figure 3. Infrared spectra of n-$C_{27}H_{56}$ in the solid phases I (20 °C) and II (57 °C) and in the liquid (69 °C). Bands present in phase II which are not found in phase I are marked by single asterisks; if these bands are also found in the liquid, they are marked by double asterisks. Spectra were recorded with the same sample pathlength. The absorbance scale (arbitrary units) for the liquid spectrum has been reduced by a factor of 2 with respect to the solid spectra.

related to the relative phase difference between the motions of adjacent methylene groups along the chain.[21] For the isolated all-trans conformer, only the k-odd members of the rocking progression are infrared active, and indeed only odd members appear in the low-temperature spectrum. Due to the nonlocalized nature of this type of vibration, the number, the frequencies, and the intensities of the bands in a progression are dependent on both chain length and chain conformation.

The second type of vibration involves motions that are localized in certain parts of the chain. The methyl rocking mode at 890 cm^{-1} (labeled P_{CH_3} in Figure 2) is an example of a localized vibration. The frequencies of these vibrations are dependent only on local conformation and, in contrast to nonlocalized modes, tend to be independent of both chain length and the conformation of the rest of the molecule.

A characteristic feature of the spectra of odd-numbered n-alkanes in phase I is the doubling of some bands, especially the rocking-mode bands, for example P_{11}, P_{19}, and P_{21} in Figure 2. This doubling arises from the factor-group splitting of modes in the orthorhombic unit cell and is a consequence of intermolecular coupling.[22,24]

The IR spectra of C_{27} in solid phases I and II and in the liquid state are compared in Figure 3. The differences between these spectra are typical of the other n-alkanes studied. The spectrum of the high-temperature phase II is intermediate in appearance between the spectra of phase I and the melt. Whereas the well-defined bands in the low-temperature-solid spectrum result from a single molecular conformation, the broad features of the liquid spectrum are due to the superposition of bands from an enormous number of different conformers. In the liquid, bands

(24) R. G. Snyder, *J. Chem. Phys.*, **71**, 3229 (1979).

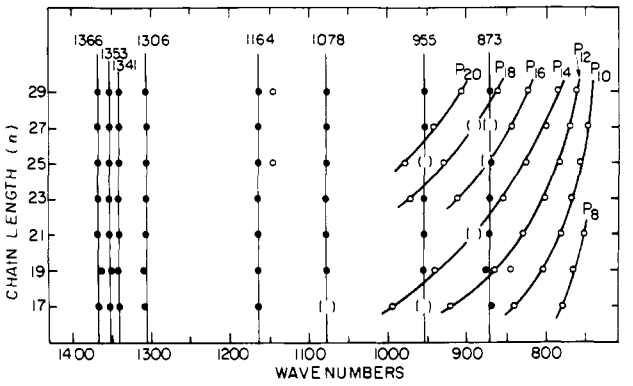

Figure 4. New bands observed in the phase II spectra of odd n-alkanes, C_n. Constant-frequency bands are denoted with shaded circles and their average frequency is given at the top of the figure. Bands whose frequencies are chain-length dependent are denoted by open circles. They are assigned to k-even rocking modes (P_k) as indicated. Parentheses indicate the presence of extraneous bands that obscure bands belonging to this array.

due to nonlocalized rocking and wagging progressions tend to overlap to form a continuous background, and for this reason localized modes account for most of the bands observed. Localized bands in the liquid spectrum include the CH_3 rocking band (890 cm^{-1}) also present in phase I, together with new bands which are associated with CH_2 wagging modes localized at specific nonplanar conformational sequences.[23]

In general, the appearance of the spectrum of phase II suggests that the degree of conformational order present in this phase lies somewhere between the extremes presented by the liquid and solid I phases. In contrast to the liquid, most bands belonging to the rocking and wagging progressions of all-trans molecules are still identifiable in the spectrum of phase II. However, these bands are broader than those in phase I, and their intensity is greatly reduced. Factor-group splitting is absent or much diminished in phase II. Most significantly, there are bands in the spectrum of phase II that do not appear in the spectrum of phase I and that are not attributable to vibrations of all-trans conformers. These are marked with asterisks in Figure 3. The frequencies of some of these new bands (double asterisks) are nearly identical with those of bands in the liquid spectrum that are characteristic of localized vibrations. Thus, while the all-trans molecules are still a major component of phase II, nonplanar molecules are clearly in evidence.

B. Normal Coordinate Assignments. The frequencies of the bands that we have observed in phase II but not in phase I are summarized in Figure 4. Chain-length-dependent and constant-frequency bands are both present. As noted earlier, these two types of modes correspond respectively to nonlocalized and localized vibrations. To identify the specific conformations associated with these bands, we have calculated frequencies and normal coordinates for n-alkanes having different chain lengths and a variety of conformations. Details of the computational methods and force field used in these calculations have been previously described.[21,23]

First we consider the chain-length-dependent bands that appear in the rocking-mode region ($\sim$1000–750 cm^{-1}) in phase II. The new bands in this region occur approximately midway between the k-odd rocking-mode bands associated with the all-trans conformation and consequently have frequencies that correspond to k-even rocking modes. Since the k-even modes are IR inactive for the all-trans chain, these bands must result from a nonplanar conformation. However, their closeness to the calculated all-trans frequencies suggests a conformation not much different from the planar chain. Our calculations indicate that the frequencies and relative intensities of these bands are best accounted for by the end-gauche conformation. In this conformation the penultimate bond of the chain is in the gauche state (g or g′) while the remaining bonds are trans (t). This conformer may be denoted as gt_{n-4} where n refers to the total number of C atoms in the chain.

Table III. Frequencies and Description of Constant-Frequency Modes Associated with Nonplanar Conformers in Phase II

	$\bar{\nu}_{obsd}$, cm^{-1}	$\bar{\nu}_{calcd}$, cm^{-1}	description of mode	m^a
end-gauche (gt_m)	1341	1345	CH_2 wag	$m \geq 1$
	1164	1167	CH_2 rock, CH_3 rock	$m > 1$
	1078	1079	CH_2 wag, C–C stretch	$m > 1$
	955	960	CH_3 rock, C–C stretch	$m > 8$
	873	878	CH_3 rock, C–C stretch	$m > 5$
kink ($t_m(gtg')t_m^*$)	1366	1367	CH_2 wag	$m, m^* \geq 0$
	1306	1313	CH_2 wag	$m, m^* \geq 0$
double gauche ($t_m(gg)t_m^*$)	1353	1354	CH_2 wag	$m, m^* \geq 0$

[a] Degree of localization. The estimated values of m represent the minimum number of trans bonds needed so that, if the $(m + 1)$th bond is gauche, the frequency of the localized mode will be within 5 cm^{-1} of the limiting frequency for large m.

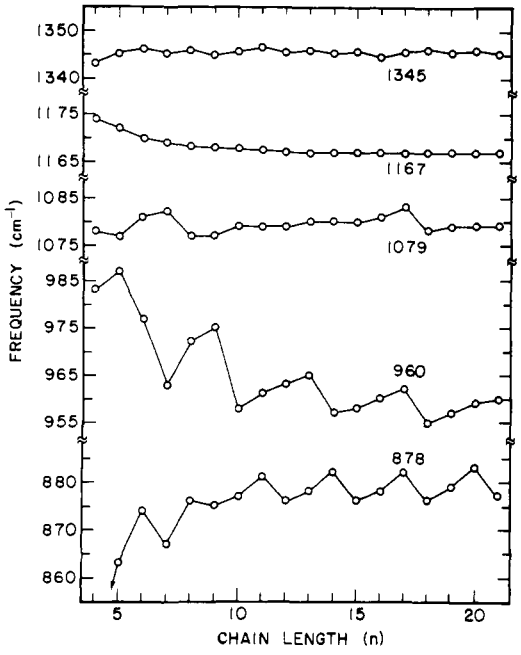

Figure 5. Calculated frequencies of the localized modes of the end-gauche conformation (gt_{n-4}) as a function of chain length for n-alkanes C_n.

Most of the constant-frequency bands (Figure 4) can also be assigned to the end-gauche conformation. The observed and calculated frequencies of the constant-frequency modes are summarized in Table III. The observed frequencies are in excellent agreement with those calculated for the end-gauche conformer. Moreover, all vibrations of this conformation that would be expected to be infrared intense on the basis of a simple group moment model[25] are indeed observed in the phase II spectrum.

In reality, "localized" modes vary to some extent in their degree of localization. Some measure of localization is provided by the integer m which is given a value in Table III for each vibration. The meaning of m is appropriately illustrated by the end-gauche conformation. If we designate this conformation by gt_l, where l is the number of adjacent trans bonds, and designate the frequency of a localized mode associated with this conformation by $\nu(gt_l)$, then m has a value such that $|\nu(gt_\infty) - \nu(gt_m)| < 5$ cm^{-1}. For the end-gauche defect, m ranges from 1 to 8 depending on the vibration (Table III).

The frequencies of the localized modes are slightly dependent on the length of the chain even for very long chains. This is illustrated in Figure 5, where we have plotted the frequencies calculated for the localized modes of the end-gauche conformer gt_{n-4} against chain length n. The localized modes show a small periodic variation in frequency with chain length. This behavior is the result of an interaction between the given localized mode, whose frequency is essentially constant, and nonlocalized modes whose frequencies are chain-length dependent. The interaction is greatest when the frequencies of the two kinds of modes are closest. Since nonlocalized modes always occur in series, the effect of increasing the chain length is to parade members across the constant-frequency (localized) mode thus causing its frequency to be perturbed in a regular cyclic manner. The most localized vibrations are least affected by this kind of interaction of course.

(25) R. G. Snyder, *J. Chem. Phys.*, **42**, 1744 (1965).

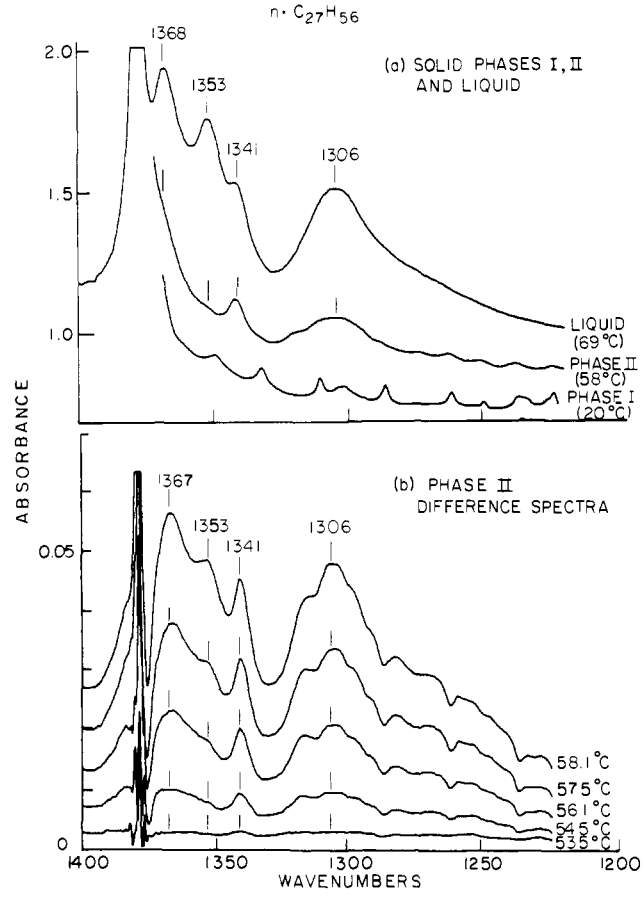

Figure 6. Infrared spectra of n-$C_{27}H_{56}$ in the wagging-mode region. (a) Solid phases I (20 °C) and II (58 °C), and the liquid (60 °C). The absorbance scale of the liquid spectrum has been reduced relative to that of the solid spectra. (b) Difference spectra of the solid in phase II as a function of temperature. In each case we have subtracted a reference spectrum measured with the sample at a temperature (53.3 °C) just above the α transition (T_α = 53.3 °C and T_{mp} = 58.8 °C from DSC measurements).

Finally, we note that the existence of constant-frequency bands characteristic of the conformational sequence gt_m... provides no information about the conformation of the rest of the molecule. However, the presence of the P_{even} bands, which are associated with the nearly all-trans chain, suggests that many of the end-gauche defects occur in otherwise planar chains.

Besides the end-gauche defect, other nonplanar conformations are indicated by certain constant-frequency bands that occur in the wagging-mode region. Figure 6 shows this region for C_{27}. In Figure 6a we compare the spectra of solid phases I and II and the liquid. Figure 6b shows a series of difference spectra within phase II as a function of temperature. The difference spectra are useful because they emphasize those features that change with temperature.

The new bands in the methylene wagging region of phase II correspond in frequency to bands in the spectrum of the liquid that have been previously assigned to localized vibrations associated with short sequences of bonds having a specific conformation.[23]

These assignments are given in Table III. The band at 1341 cm^{-1} belongs to the end-gauche conformation. The shoulder at 1367 cm^{-1} and the broad band at 1306 cm^{-1} have been shown to result from conformational sequences gtg or gtg′ in the liquid. On the basis of packing considerations, it seems reasonable to exclude the presence of the gtg sequence in the solid. A gtg′ defect can be much more readily incorporated into the solid since such a sequence in an otherwise trans chain connects two parallel but laterally displaced trans segments.

The gtg′ defect was first postulated to exist in phase II by Blasenbrey and Pechhold.[14] In their "kink-block" model, gtg′ defects were envisioned to occur with equal probability anywhere along the chain. Our spectra support this model.

The argument for a distribution of kinks along the chain rests in the fact that, if we assume a random distribution, we can account for the observed shape of the low-frequency shoulder of the 1306-cm^{-1} band. This shoulder cannot be accounted for, however, if the kinks are concentrated at only a few sites. To demonstrate this we have calculated spectra of C_{16} molecules containing a single gtg′ kink at various chain positions. In an earlier study of liquid *n*-alkanes,[23] it was found that nearly all the infrared intensity of bands associated with localized wagging modes originates from the methylene groups adjoining gauche bonds. In calculating the spectra of these conformers, we have therefore assumed that the intensity of the wagging mode originates in the displacement of the wagging coordinates of the two methylene groups that are connected by the trans bond of the kink.

The calculated spectra of the series of C_{16} conformers having kinks at different sites are displayed in Figure 7a. A common feature in all spectra is the intense band at 1313 cm^{-1} due to the methylene wagging mode which is approximately localized within the kink. Less localized wagging modes contribute intensity at lower frequencies and give rise to bands whose frequencies are dependent on the specific site of the kink. We note that the band observed at 1306 cm^{-1} does not have well-defined structure on the low-frequency side and in this respect does not resemble the spectrum calculated for any one specific kink conformer.

The calculated spectrum which results from summing these individual conformer spectra is shown in Figure 7b. The calculated spectrum includes all the spectra in Figure 7a, each given equal weight, together with the spectrum of the conformer tgt_{11}. The latter conformer is in effect another kink form in the sense that a trans pair of methylenes is isolated by the gauche bond and the methyl group, and its calculated spectrum is similar to those of the other kink conformers. The observed spectrum of C_{27} in phase II is also shown in Figure 7b. Given the simplicity of the present calculation, the similarity in peak position and overall shape between the observed and calculated bands is remarkable. The effect of summing the individual kink spectra is to give the 1313-cm^{-1} band an extended, featureless tail on the low-frequency side that closely mimics the observed tail. Thus, we conclude that the entire 1306–cm^{-1} band observed in phase II can be explained on the basis of kink conformers alone. Further, the intensity pattern implies that kink defects are distributed over a large number of chain sites rather than at just a few.

For completelness, we have included in Figure 7b the spectrum of C_{27} in the liquid state. Whereas most features of this spectrum differ from that of phase II, the shape of the 1306-cm^{-1} band is similar. Perhaps this is not surprising given the following. Both gtg′ and gtg defects are present in the liquid; these defects are randomly distributed; earlier calculations[23] indicate that other kinds of defects do not contribute bands in this frequency region. A calculation of the spectrum of the liquid would probably show that the shape of the 1306-cm^{-1} band is not sensitive to the details of the conformational disorder.

Finally, a constant-frequency band is observed at 1353 cm^{-1} in the spectrum of phase II. This band is characteristic of the local sequence gg (double-gauche) and is prominent in the spectrum of the liquid (Figure 6a) being of comparable intensity to the 1341-cm^{-1} end-gauche band. In contrast, in phase II, the 1353-cm^{-1} band is weak and appears distinctly only when the sample is within 1–2 °C of its melting point. Difference spectra

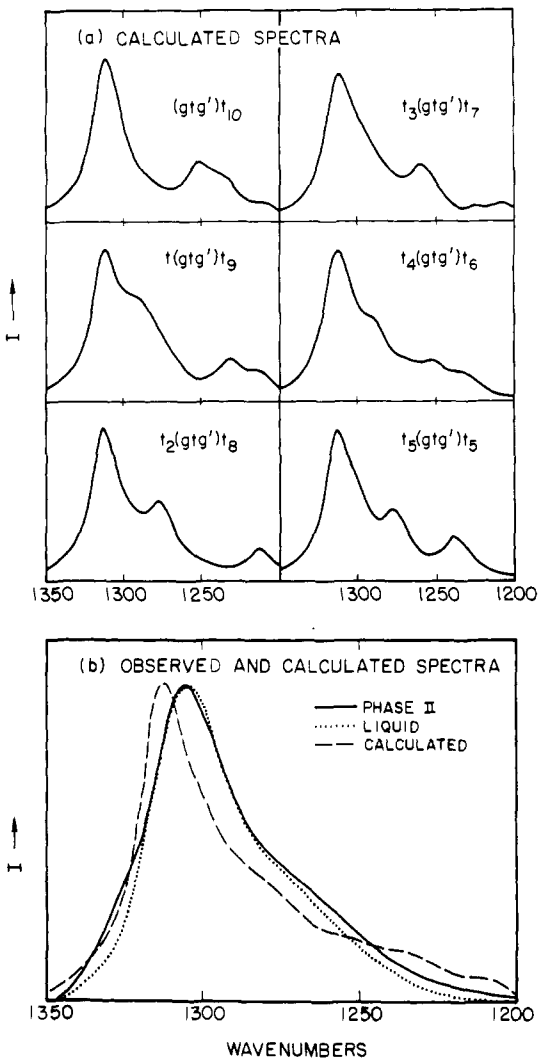

Figure 7. Calculated and observed IR spectra in the region of the 1306-cm^{-1} band. (a) Spectra calculated for the conformers of *n*-$C_{16}H_{34}$ having one gtg′ kink per chain. For each conformer, the intensity contributed by a normal mode was assumed to be proportional to $(W_\alpha + W_\beta)^2$ where W_α and W_β are the **L**-matrix elements of the CH_2 wagging coordinates associated with CH_2 groups (α and β) connected by the trans bond of the gtg′ defect. These modes were then represented by Lorentzian bands with fwhh = 20 cm^{-1}. All bands of a given conformer were summed to produce the spectrum shown. (b) Spectra of *n*-C_{27} in phase II and in the liquid phase and the calculated spectrum obtained by summing the spectra above. All calculated spectra were given equal weight, and the spectrum of the tgt_{11} conformer (not shown) was also included in the summation. The 1353- and 1341-cm^{-1} bands, which are not associated with kink defects, are not included in the observed spectra. The shape of the 1306-cm^{-1} band for solid phase II was obtained by smoothing the difference spectra (Figure 6b) to remove the dips that result from the all-trans wags whose intensity decreases in this phase.

(Figure 6b) reveal, however, that this band and therefore some gg sequences are indeed present throughout phase II. The relative intensity of the 1353-cm^{-1} band indicates that gg sequences represent only a small fraction of the nonplanar forms except perhaps very close to the melting point. This point will be discussed further in the following section.

We conclude this section by considering what the presence of the nonplanar conformers identified in phase II may imply about the structure of this phase. The three types of defects observed are shown in Figure 8 along with the all-trans conformer.

The predominant conformers in phase II are the planar form and the nonplanar forms that contain end-gauche and kink defects. It is significant that, if these two defects are placed in an otherwise planar chain, the overall shape of the all-trans molecule tends to be preserved. This is not true in the case of most other nonplanar conformations such as found in the liquid. Thus, the conforma-

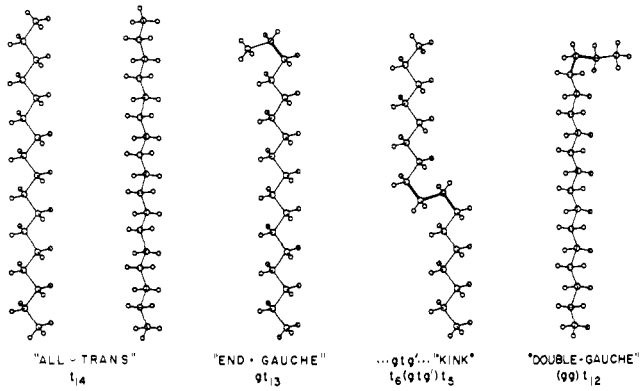

Figure 8. Structures of the planar conformer and of the nonplanar conformations observed in phase II. Defects (bold face) are shown in chains of C_{17} that are otherwise planar.

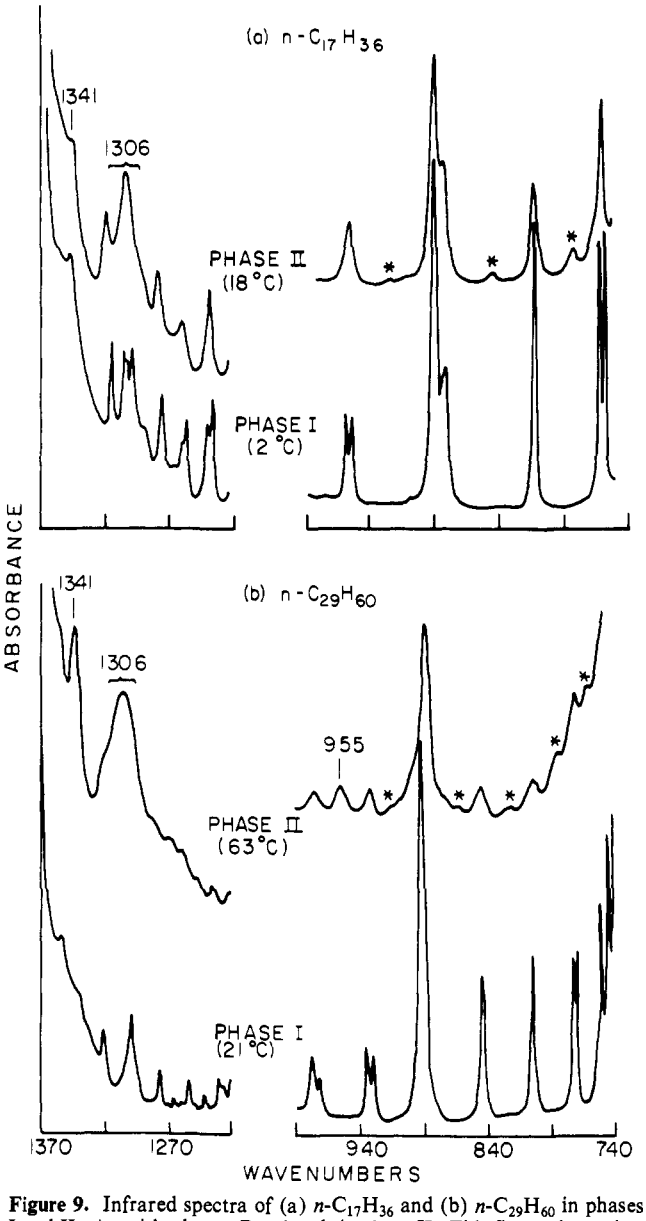

Figure 9. Infrared spectra of (a) n-$C_{17}H_{36}$ and (b) n-$C_{29}H_{60}$ in phases I and II. Asterisks denote P_{even} bands in phase II. This figure shows that the differences between the spectra of phases I and II are larger for C_{29} than for C_{17}.

tional disorder present in phase II is not liquidlike. Rather, it appears that this disorder is specifically compatible with a structure similar to that of phase I in which the parallel arrangement of chains is maintained. Of course, end-gauche defects in phase II disrupt the packing between lamellae while kink defects within chains disrupt the lateral packing of chains relative to the highly ordered packing of phase I.

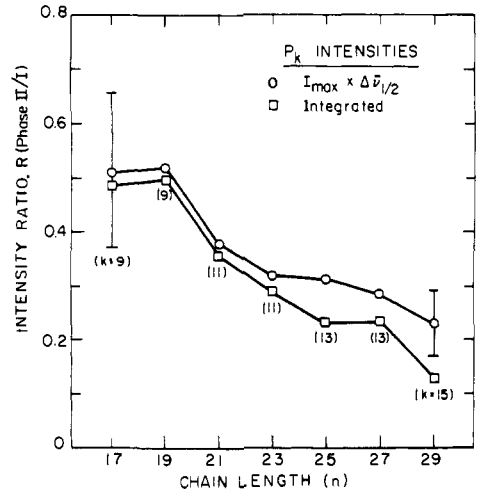

Figure 10. Ratio of intensity of P_{odd} bands in phase II to the corresponding bands in phase I as a function of chain length, C_n. R is the ratio of the phase II intensity for the sample 1 °C below the melting point to the phase I intensity 20 °C below the melting point. The two sets of data refer to intensities measured by integration (squares) and by the product of peak intensity and half-width (circles). The band chosen for each n-alkane corresponds to the rocking mode, P_k, that is closest in frequency to 800 cm^{-1}; the value of k, which indicates the assignment, is given in parentheses below each data point. Error bars reflect an estimated uncertainty of ±20% in the measured intensities.

The other defect identified in phase II is the double-gauche sequence. A gg defect in an otherwise planar chain causes a roughly 90° bend in the molecule which would be highly disruptive of packing unless the defect were placed at the end of the chain as shown in Figure 8. In this case, the resulting conformer resembles the end-gauche form. Even so, the very small concentration of double-gauche defects in phase II relative to end-gauche and kink defects indicates that these defects are not favored in the solid. This is further evidence that the conformational disorder in the solid is unlike that in the liquid.

C. Quantitative Trends with Chain Length. The same types of conformational defects appear to exist in all n-alkanes in phase II. However, their concentration increases significantly with increasing chain length. This trend is apparent in Figure 9, where the IR spectra of phases I and II of C_{17} and C_{29} are compared. The spectra of the two phases are more nearly alike for C_{17} than for C_{29}. The decrease in the intensity of the P_{odd} bands, which are characteristic of all-trans chains, is much larger for C_{29} in going from phase I to phase II. Moreover, in phase II, the intensities of the 1341- and 1306-cm^{-1} bands, which arise from nonplanar molecules, are greater for C_{29} than for C_{17}.

The intensity ratios of certain P_{odd} bands of phase II to those of phase I are plotted as a function of chain length in Figure 10. To compare intensities of bands associated with similar kinds of vibrational motion we have selected P_{odd} bands for different n-alkanes that are near in frequency and therefore similar in form.[22] Figure 10 is based on P_{odd} bands that have frequencies near 800 cm^{-1} but the trend indicated in this figure is also found in plots that use other P_{odd} bands. Two sets of intensity data are plotted in Figure 10. These correspond to intensities evaluated in slightly different ways: (i) from direct integration and (ii) from the product of peak intensity and half-width. The product curve is consistently higher, and this suggests that some intensity is lost in the case of direct integration as a result of band broadening and overlapping. Both plots, however, indicate that there is a large loss of intensity in going from phase I to phase II and that this loss increases with increasing chain length.

The decrease of the intensity of the P_{odd} modes in going from phase I to phase II does not appear to be a good measure of the fraction of molecules that remain planar in phase II. This is especially the case for the shorter chains. For example, on this

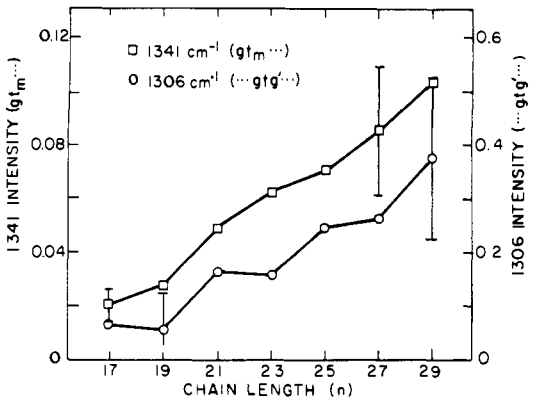

Figure 11. Relative intensities of the 1341-cm^{-1} (squares) and 1306-cm^{-1} (circles) bands in phase II 1° below the melting point as a function of chain length, C_n. Integrated intensities were ratioed to the intensity of the methyl rocking mode (P_{CH_3}, 890 cm^{-1}) in phase I to account for variations in sample thickness. For the 1306-cm^{-1} band, we have subtracted out the contribution to the intensity due to wagging-mode bands of the all-trans conformation. Error bars reflect an estimated error of ±20% in the measured intensities.

Table IV. Estimated Defect Concentrations in Solid Phase II of n-$C_{27}H_{56}$ based on a Comparison of Band Intensities in Solid II vs. Liquid Spectra

defect	$\bar{\nu}$, cm^{-1}	r(solid II/liquid)[a]	$\bar{n}_{liquid}$[b]	$\bar{n}_{solid\ II}$[c]
gt...	1341	0.24–0.48	0.624	0.15–0.30
...(gtg')...	1306	0.15–0.25	2.55	0.38–0.64
...(gg)...	1353	≤0.001	2.34	≤0.002

[a] r is the intensity ratio of the localized wagging-mode band in the spectrum of phase II to that of the liquid. [b] $\bar{n}_{liquid}$ is the average number of defects of a given type calculated for liquid C_{27} (~70 °C) based on the rotational isomeric state model as described in ref 27 and using a gauche–trans energy difference of 500 cal/mol. [c] $\bar{n}_{solid\ II}$ were obtained from the equation $\bar{n}_{solid\ II} \simeq r\bar{n}_{liquid}$.

basis the concentration of planar conformers in phase II of C_{17} and C_{19} is estimated to be about 50%. This number is significantly lower than estimates from another method that we consider reliable and which will be described presently. Factors other than changes in the conformer concentrations appear to contribute to the observed loss of intensity in these bands in going to the high-temperature phase.[26]

The intensities of bands associated with nonplanar molecules in phase II increase with increasing chain length. This may be seen in Figure 11, where the intensities of the 1341-cm^{-1} end-gauche band, and the 1306-cm^{-1} band assigned to kink conformers, are plotted against chain length. To account for variations in sample thickness, the intensities have been normalized by ratioing to the intensity of the constant-frequency methyl rocking band (890 cm^{-1}). Both the 1341- and 1306-cm^{-1} band intensities increase by a factor of 5–6 in going from C_{17} to C_{29}. The concentrations of nonplanar forms in phase II appear to increase approximately linearly with chain length.

A rough estimate of the defect concentrations may be obtained by comparing the intensities of the characteristic wagging-mode bands (1341, 1306, and 1353 cm^{-1}) in the spectrum of phase II with the intensities of these same bands in the liquid phase spectrum. The intensities are assumed to be unaffected by the state of the sample. The experimentally measured intensity ratios, solid to liquid, can be used to determine the concentration of conformational defects in phase II, since the defect concentration

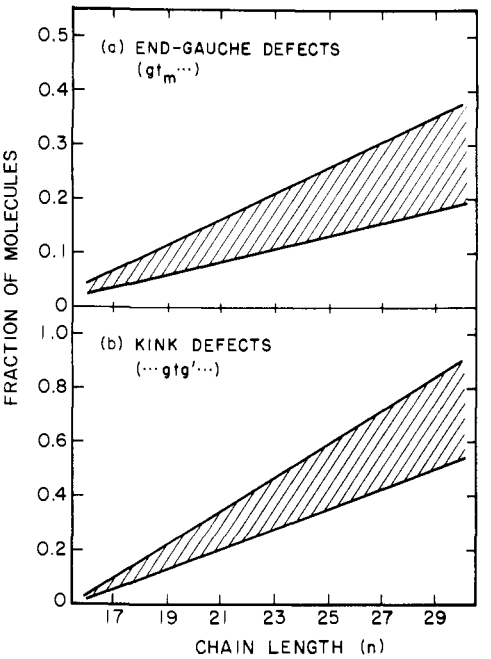

Figure 12. Estimated concentrations of (a) end-gauche and (b) kink defects in phase II vs. chain length, C_n. Concentrations were calculated from the estimated defect concentrations for C_{27} (Table IV) by fitting the intensity data of Figue 11 linearly with chain length. Defect concentrations are expected to lie within the shaded regions whose boundaries were determined by the C_{27} calculation summarized in Table IV.

in the liquid can be calculated.[27] The relevant data used in such an analysis in the case of C_{27} are summarized in Table IV. The ratios, r, of the intensities of the 1341-, 1306-, and 1353-cm^{-1} bands in solid phase II to those in liquid C_{27} are listed. Due to the uncertainties in measured intensities, a range of values for r is given. The $\bar{n}$ are the average number of defects per molecule of C_{27}. For the liquid, the $\bar{n}$ were calculated on the basis of the rotational isomeric state model (see, for example, ref 27), using an effective gauche–trans energy difference of 500 cal/mol.[28]

The estimated defect concentrations for C_{27} in phase II are roughly consistent with estimates based on the loss of intensity of P_{odd} modes. Both methods indicate that a large fraction of the molecules are nonplanar in phase II. The double-gauche defect exists in only very low concentrations, ≤0.2%. On the other hand, end-gauche and kink defects each appear in about 20–50% of the C_{27} molecules.

We are now in a position to estimate defect concentrations for other n-alkanes in phase II since the above results for C_{27} provide a reference. For simplicity, we have made the approximation that defect concentrations and chain length are linearly related as suggested by Figure 11. The estimated concentration of end-gauche and kink defects for the odd n-alkanes C_{17}–C_{29} in phase II are shown in Figure 12. (The double-gauche defect is not included because its concentration is small, less than 1% in all cases.) The two boundary lines in each plot in Figure 12 correspond to the limiting values of r given in Table IV. The actual concentrations of defects are expected to lie in the shaded regions. The concentrations of nonplanar conformers vary from small values (5–10%) for C_{17} to large values (up to about 70%) for C_{29}.

We now compare these results with previous estimates of defect concentrations. Based on IR studies, Zerbi et al.[18] concluded that end-gauche defects occurred for 10–15% of the molecules of C_{19} in phase II, a value that is only slightly higher than ours for this n-alkane. However, these authors did not detect kinks. From X-ray measurements on C_{33}, Strobl and co-workers[16] estimated that in phase II 40–70% of the chains contain a kink defect, an estimate that is in line with our results (Figure 12).

(26) Intermolecular changes that occur in the phase transitions could also affect the intensities of these modes. For example, we have observed a significant decrease in intensity of the rocking fundamental (720 cm^{-1}) of crystalline polyethylene with increasing temperature over a range (10–300 K) where no appreciable intramolecular changes are expected. R. A. MacPhail, R. G. Snyder, and H. L. Strauss, unpublished.

(27) P. J. Flory, "Statistical Mechanics of Chain Molecules", Interscience, New York, 1969.

(28) J. R. Scherer and R. G. Snyder, *J. Chem. Phys.*, **72**, 5798 (1980).

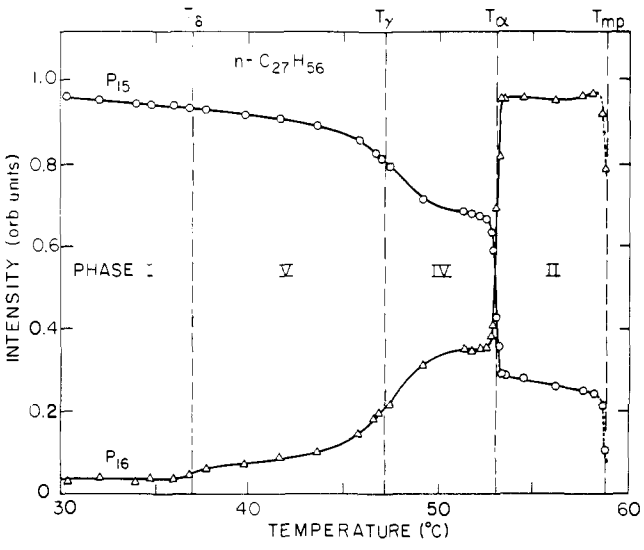

Figure 13. Integrated intensities of two rocking-mode bands of n-$C_{27}H_{56}$ as a function of temperature: (circles) P_{15} (826 cm^{-1}) and (triangles) P_{16} (845 cm^{-1}). P_{16} is plotted on an intensity scale that is 7.5 times that for P_{15} (arbitrary units). Transition temperatures marked at the top of the figure are those obtained from DSC measurements.

D. Conformational Changes at the Phase Transitions. For chains C_{25}–C_{29}, the change from phase I to phase II takes place through a sequence of three phase transitions (δ, γ, α) so that there exist two phases (V, IV) intermediate between I and II. The IR spectra of these n-alkanes change discontinuously at each of these transitions and the relative magnitudes of these changes are roughly proportional to the transition enthalpies.

Spectra of the four solid phases of C_{27} are shown in Figure 15. In the rocking-mode region, shown here, the changes that occur between successive phases (I → V → IV → II) are qualitatively similar. The P_{odd} bands decrease in intensity at each phase change, while the intensities of bands assigned to P_{even} modes of the end-gauche form increase. The temperature dependence of the intensities of P_{15} and P_{16} are plotted in Figure 13. The transition temperatures marked on this figure are those obtained from DSC measurements.

A number of general observations can be made on the basis of Figure 13 and analogous plots for the other n-alkanes. Some bands associated with the end-gauche conformer, for example, P_{16} here, have measurable intensity at temperatures well below the lowest-temperature phase transition. Thus, a small fraction of molecules are nonplanar even in the lowest-temperature solid phase. With increasing temperature, the IR spectra show discontinuous changes corresponding to abrupt jumps in the concentrations of nonplanar forms at *each* phase transition. The concentration of nonplanar forms is not constant in a given phase. Rather, within each phase their concentation gradually increases with increasing temperature, although the increase is generally small relative to that at phase transition.

We now consider how the concentrations of the various defects change in going through the phase transitions. The concentration of the end-gauche defect is easiest to monitor because several of its characteristic bands have a high intrinsic intensity and lie in spectral regions devoid of interfering bands. It is clear that some end-gauche molecules are present in each phase. From the temperature dependence of the relative intensities of P_{even} modes, such as shown in Figure 13, we find that the increase in the concentration of end-gauche defects at the δ transition (and thus their concentration in phases I and V) is only a few percent of the concentration of these defects in phase II. However, the change in concentration at the γ transition is much larger than at δ. In fact for C_{27} and C_{29}, where the γ and α transitions are well separated, the change in the concentration of end-gauche defects at the γ transition is only slightly less than that at the α transition.

It is more difficult to detect the presence of other kinds of nonplanar conformers in the lower-temperature phases. The bands

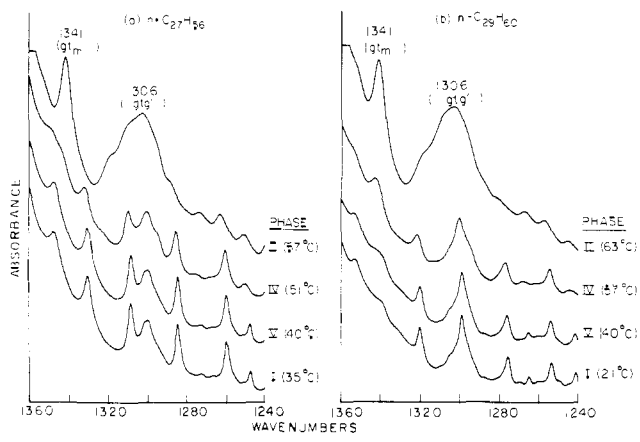

Figure 14. Infrared spectra in the wagging-mode region for the four solid phases of (a) n-$C_{27}H_{56}$ and (b) n-$C_{29}H_{60}$.

that identify double-gauche and kink defects occur in the 1380–1200-cm^{-1} region of the spectrum, which is densely populated with wagging-mode bands of the all-trans conformer. The spectra of the four solid phases of C_{27} and C_{29} in this region are shown in Figure 14.

We find no evidence for the presence of the 1353-cm^{-1} band of the double-gauche defect in the low-temperature phases of C_{27} and C_{29} (Figure 13). This is not surprising since the concentration of this defect is small in phase II and would be expected to be significantly smaller in the lower-temperature phases.

The presence of kinks is manifest in the broad band at 1306 cm^{-1} which is clearly evident in the spectrum of phase II shown in Figure 14. The integrated intensity over the frequency region (1330–1270 cm^{-1}) encompassing the 1306-cm^{-1} band appears to remain constant in passing through the δ transition (I → V). At the γ transition (V → IV), however, there is a slight increase which amounts at most to 5–10% of the intensity of the 1306-cm^{-1} band in the spectra of phase II. Whether this small intensity gain is in fact due to the presence of kinks or results from other changes occurring at the γ transition is difficult to determine. In any event, the relative increase in intensity is much smaller than that observed in the case of the end-gauche bands. We thus conclude from these measurements that, while some kink defects may be formed at the γ transition, the paramount conformational change is the formation of end-gauche, not kink, defects.

An important difference therefore between the α transition and the lower-temperature transitions is in the kinds of conformational defects involved. The formation of end-gauche defects appears to be a disordering process that is common to all phase transitions, whereas kink defects are formed predominantly, or possible exclusively, at the α transition. Thus, the lower-temperature transitions involve mainly a disruption of the packing of chain ends between molecular layers. While disruption of this sort occurs also at the α transition, there is in addition a disordering of the packing of chains in their interior regions as a result of the formation of kinks.

Another source of structural information which supports this interpretation is the behavior of the factor-group splitting of methylene rocking-mode bands. Changes in the splitting for the different phases of C_{27} may be seen in Figure 15. The δ transition has the least effect on the splitting, indicating only a small change in molecular packing, which is, of course, not unexpected considering the small value of ΔH_δ. At the γ transition, the splitting of the higher-frequency members of the rocking-mode progression is reduced while lower-frequency bands are much less affected. In fact, the splitting of the lowest-frequency member of the series (P_1, not shown) is virtually unchanged at either the δ or γ transitions. Only at the α transition does the splitting of the lowest-frequency rocking bands collapse or nearly collapse.[29]

(29) H. L. Casal, D. G. Cameron, H. H. Mantsch, and R. G. Snyder, *J. Chem. Phys.*, 77, 2825 (1982).

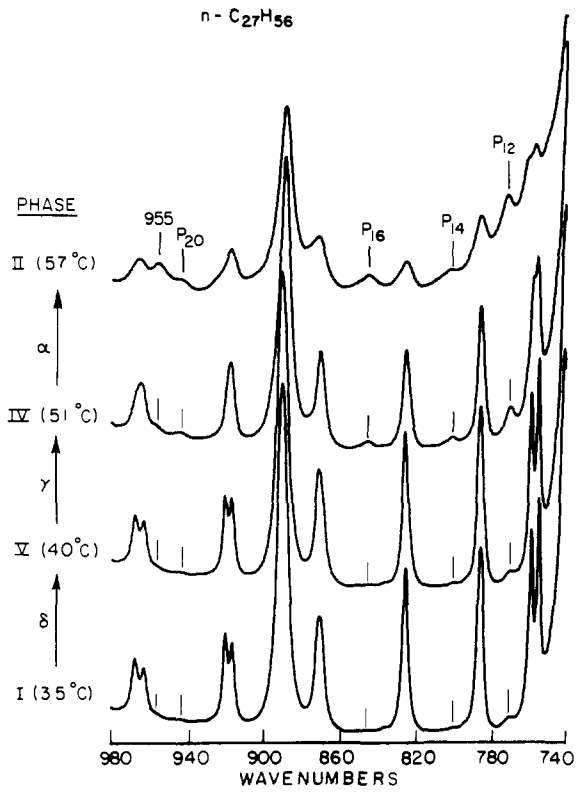

Figure 15. Infrared spectra in the rocking-mode region of the four solid phases of n-$C_{27}H_{56}$. For clarity, only the P_{even} bands are labeled. The intense band at 890 cm^{-1} is the methyl rocking mode and the remaining bands, except the 955-cm^{-1} end-gauche band, are P_{odd} modes. Note the presence of P_{even} bands in all four phases. (The transition temperatures determined by DSC measurements are T_δ = 36.6 °C, T_γ = 47.6 °C, T_α = 53.3 °C, and T_{mp} = 58.8 °C.)

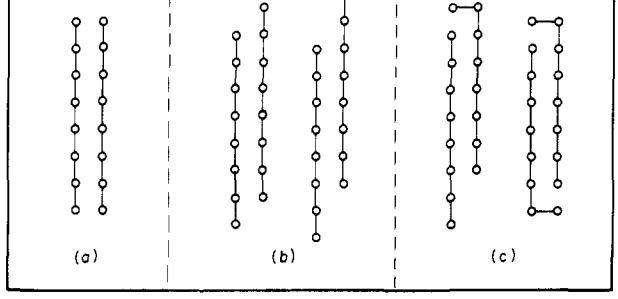

Figure 16. Schematic representations of (a) orthorhombic chain packing in phase I, and (b, c) possible variations of this packing. In b the chains are shown longitudinally displaced by one and two methylene units; c represents possible packing schemes that accommodate end-gauche defects.

This difference in behavior of the factor-group splitting of high-frequency vs. low-frequency rocking modes is a consequence of the short-range nature of the interchain interactions that give rise to the splitting.[22,30] The effect of longitudinal displacements of adjacent chains on the splitting pattern is analyzed in ref 24. The situation is illustrated in Figure 16, which shows the orthorhombic structure (Figure 16a) along with structures in which there is a longitudinal displacement of chains (Figure 16b). Calculations on a model system[24] indicate that such longitudinal displacements do not affect the factor-group splitting of bands near the 720-cm^{-1} (P_1) limit but do markedly affect splitting of the higher-frequency bands. Packing rearrangements that could accommodate the inclusion of end-gauche defects, such as shown

(30) M. Tasumi and T. Shimanouchi, *J. Chem. Phys.*, **43**, 1245 (1965).

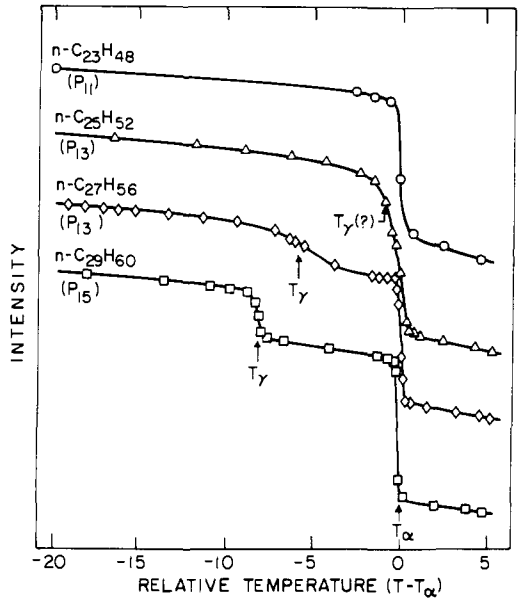

Figure 17. Integrated intensities of P_{odd} bands as a function of temperature for n-$C_{23}H_{48}$ and n-$C_{25}H_{52}$, n-$C_{27}H_{56}$ and n-$C_{29}H_{60}$. The temperature scales have been shifted so that $T_\alpha \equiv 0$ for each n-alkane. The T_γ transition temperatures for C_{27} and C_{29} were obtained from DSC measurements. For C_{25}, an indication of the γ transition is found in the initial gradual change in this curve before the α transition. The curves have been vertically displaced for clarity.

in Figure 16c, would be expected to affect the splitting pattern in a similar manner. Therefore, the introduction of end-gauche defects and the longitudinal disorder that results could lead to the loss of splitting of the higher-frequency rocking bands without changing the splitting of the lowest-frequency bands.

On the other hand, conformational disorder within the chain, such as that associated with kinks, will result in a disruption in *lateral* packing of chains. As a consequence, the short-range vibrational coupling between chains that gives rise to the factor-group splitting will also be disrupted. In contrast to the effect of longitudinal displacement, lateral disorder will affect the splitting of all modes. The observed behavior of the factor-group splitting thus can be explained in terms of the formation of end-gauche defects at the δ and γ transitions and the formation kink defects at the α transition. However, we note that increases in lateral unit cell dimensions and in orientational disorder are closely related to, and produce effects indistinguishable from, the formation of kink defects.

We finish with a few remarks concerning the sharpness of the phase transitions. For all of the n-alkanes C_{17}–C_{29}, with the exception of C_{25} which will be considered below, the α transition occurs over a narrow temperature interval of 0.2–0.4 °C. All of the other transitions are somewhat broader. The δ transition, which is by far the weakest, takes place over a relatively wide interval, roughly 2 °C.

The width of the γ transition shows an interesting dependence on chain length. This is illustrated in Figure 17, where we have plotted the integrated intensities of certain P_{odd} bands against temperature for C_{23}–C_{29} The temperature scales have been shifted for each n-alkane so that T_α is always at zero. The figure shows both the α and γ transitions. For C_{29}, where T_γ is about 8 °C below T_α, the γ transition occurs over a narrow temperature interval of ~0.8 °C. For C_{27}, in which case T_γ and T_α are closer together, the γ transition is much broader, extending over a range of 4–5 °C. However, the α transition remains sharp. Finally, for C_{25}, α and γ appear to merge. A perturbation due to the presence of the γ transition is indicated, however, in the broad leading edge going into the α transition (Figure 17). For C_{23} and shorter n-alkanes, the α transition is again found to be sharp and no manifestation of γ is apparent. These observations suggest that the breadth of the γ transition is linked to its eventual disappearance (or incorporation) into the α transition. This behavior

is of theoretical interest since it may signal a change in the order of the γ transition with chain length as γ and α merge.[31]

Summary and Conclusions

We have studied the solid–solid phase transitions in the odd *n*-alkanes C_{17}–C_{29} using DSC and IR spectroscopy. The major results are summarized as follows:

(1) The odd *n*-alkanes, C_{17}–C_{23}, exhibit a single solid–solid phase transition, which has been previously reported.[7] However, C_{25}–C_{29} exhibit two additional phase transitions which were detected by DSC measurements. These latter transitions are correlated with transitions recently reported[16,17] for *n*-alkanes longer than C_{29} (Figure 1).

(2) At *every* phase transition detected by DSC, we have observed discontinuous changes in the infrared spectra. These changes result from abrupt increases in the concentrations of nonplanar conformations.

(3) The nature of the nonplanar conformations found in the solid phases of the *n*-alkanes is quite different from that in the liquid state. In the highest-temperature solid phase (II), three specific nonplanar defects were identified. These are the "end-gauche", "kink", and "double-gauche" forms. The end-gauche and kink forms are the dominant nonplanar conformers present in phase II. The double-gauche defects occur in much lower concentrations than the others although very near the melting point their concentration increases markedly.

(4) The concentrations of nonplanar conformers increase roughly linearly with increasing chain length. For C_{27} and C_{29}, the longest chains studied, we estimate that end-gauche defects occur in ~20–30% of the molecules while kink defects occur in ~60–70% of the molecules.

(5) The formation of end-gauche defects is a disordering process that is common to all of the phase transitions. Kink defects, on the other hand, seem to be formed primarily (or exclusively) at the α transition.

(6) The concentration of defects increases with increasing temperature within each phase. This increase is greatest in the highest-temperature phase as the melting point is approached but occurs in other phases as well.

(7) The sharpness of the γ transition appears to be dependent on the temperature separation between T_γ and T_α which in turn is a function of chain length. This behavior may result from some type of "interaction" between the α and γ transitions.

We return to the question raised in the Introduction—how is the defect structure of the alkane chains related to the existence of distinct solid phases? The phase diagram (Figure 1) shows an increasing number of phases as the chain length increases. We have shown that the number of defects also increases rapidly as a function of chain length until most of the chains of C_{29} are nonplanar in the highest-temperature phase. This suggests that the conformational disorder is intimately linked with the very existence of the many phases transitions. The older concept of a "rotator" phase is too simple and, in fact, for the longer chains the kink-block model[14] may be a more appropriate starting point for describing the highest-temperature phase.

It is difficult to envision the distinct kinds of long-range order that must be characteristic of the many solid phases. There seem to be some analogies to liquid crystal smectic B phases,[32] which have a layer structure with order in each layer. Various models which are either more crystallike or more liquidlike are discussed in ref 32. We emphasize that for the *n*-alkanes we need to account for at least four phases intermediate between the low-temperature solid and the liquid. The existence of these subtle ordering phenomena presents many opportunities for further study. They suggest the possibility of arriving at an overall description of "order" in *n*-alkane systems which would elucidate the structure of many chain assemblies of vital importance.

Acknowledgment. We gratefully acknowledge support from the National Institutes of Health and the National Science Foundation. M.M. has been sponsored as a Chevron Chemistry Fellow.

Registry No. *n*-$C_{19}H_{40}$, 629-92-5; *n*-$C_{21}H_{44}$, 629-94-7; *n*-$C_{23}H_{48}$, 638-67-5; *n*-$C_{25}H_{52}$, 629-99-2; *n*-$C_{27}H_{56}$, 593-49-7; *n*-$C_{29}H_{60}$, 630-03-5; *n*-$C_{16}H_{34}$, 544-76-3; *n*-$C_{17}H_{36}$, 629-78-7.

(31) The presence of impurities can also lead to a broadening of these transitions (see ref 17). The fact that the changes are systematic with chain length, that we observe the weak δ transition, and that the α transition is sharp for C_{27}, however, argues against this possibility.

(32) P. G. deGennes, "The Physics of Liquid Crystals", Oxford University Press, Oxford, 1974.

Influence of Ion Pairing on Cation Transport in the Polymer Electrolytes Formed by Poly(ethylene oxide) with Sodium Tetrafluoroborate and Sodium Tetrahydroborate

R. Dupon,[†] B. L. Papke,[†] M. A. Ratner,*[†] D. H. Whitmore,*[‡] and D. F. Shriver*[†]

Contribution from the Materials Research Center and Departments of Chemistry and Materials Science, Northwestern University, Evanston, Illinois 60201. *Received January 14, 1982*

Abstract: Vibrational spectroscopic and conductivity data for complexes of $NaBF_4$ and $NaBH_4$ with poly(ethylene oxide) indicate that extensive contact ion pairing occurs in the $NaBH_4$ complex but not in the $NaBF_4$ complex. As a result the ionic conductivity is considerably lower in the $NaBH_4$ complex due to trapping of the mobile sodium cations by the anion. Conductivity studies on mixed anion complexes of poly(ethylene oxide) containing both ion-pairing (BH_4^-) and non-ion-pairing (BF_4^-) anions suggest that cation transport in these systems is not limited by motion through the polymer helical channels in which the cation is thought to reside. Conduction between helical chains appears to be a dominant process.

Introduction

Solid materials which exhibit anomalously high ionic conductivity ($\sigma > 10^{-5}\ \Omega^{-1}\ cm^{-1}$) are referred to as fast-ion conductors or solid electrolytes. They are the topic of considerable current research both for applications to fuel cells, sensors, electrolytic cells, and high-energy-density batteries and because the mechanisms which lead to high ionic mobility in solids are of considerable intrinsic interest. Most solid electrolytes are either of framework type or of molten-sublattice type. The framework materials are hard, covalent solids (often silicates, titanates, or aluminas), which transport monocations such as Na^+, K^+, Ag^+, or Li^+. The

[†] Chemistry Department.
[‡] Materials Science Department.

0002-7863/82/1504-6247$01.25/0